Facilitated Spin Models of Dissipative Quantum Glasses

Beatriz Olmos, Igor Lesanovsky, and Juan P. Garrahan
School of Physics and Astronomy, University of Nottingham, Nottingham, NG7 2RD, United Kingdom
(Received 3 April 2012; published 10 July 2012)

We introduce a class of dissipative quantum spin models with local interactions and without quenched disorder that show glassy behavior. These models are the quantum analogs of the classical facilitated spin models. Just like their classical counterparts, quantum facilitated models display complex glassy dynamics despite the fact that their stationary state is essentially trivial. In these systems, dynamical arrest is a consequence of kinetic constraints and not of static ordering. These models display a quantum version of dynamic heterogeneity: the dynamics toward relaxation is spatially correlated despite the absence of static correlations. Associated dynamical fluctuation phenomena such as decoupling of time scales is also observed. Moreover, we find that close to the classical limit, quantum fluctuations can enhance glassiness, as recently reported for quantum liquids.

DOI: 10.1103/PhysRevLett.109.020403 PACS numbers: 05.30.−d, 05.50.+q, 61.43.Fs, 64.70.P−

Introduction.—A central problem in condensed-matter science is that of the glass transition. Many-body systems with excluded volume interactions, such as molecular liquids, experience pronounced dynamical slowdown at high densities and/or low temperatures, to the extent that they eventually cease to relax and form the amorphous solid we call glass. The glass transition as observed experimentally is not a phase transition but a very rapid kinetic arrest. At low enough temperature or high enough density, glass formers relax too slowly to be observed experimentally in equilibrium and, thus, behave as (nonequilibrium) solids. This solidification occurs in the absence of any evident structural ordering, in contrast to more conventional condensed-matter systems: in glass formers thermodynamics changes, apparently, very little but dynamics changes dramatically. Dynamic arrest like that of glasses is a generic phenomenon in condensed matter; for recent reviews see [1–4].

While the first hallmark of glass formers is kinetic arrest, the second is dynamical heterogeneity [5]. Glass formers appear structurally homogeneous, but their dynamics is highly heterogeneous: as they slow down, spatial dynamical correlations emerge and these become more pronounced the longer the relaxation times. One theoretical perspective on glasses in which dynamical heterogeneity appears naturally is that of dynamical facilitation, which posits that the origin of glassy slowing down is not to be found in thermodynamic ordering [6] but in effective constraints in the dynamics (see [2] for a review). From this perspective, slowdown, heterogeneity, and other fluctuation features of glasses are rooted in the complex structure of trajectory space. This theory has emerged from the study of a class of idealized lattice systems, so-called kinetically constrained models [7–9], of which the simplest representatives are the facilitated spin models [8–10].

Quantum glasses, just like their classical counterparts, are of much current interest, among other reasons due to their relevance to issues like supersolidity [11], quantum annealing [12], glassiness in electronic systems [13], thermalization and many-body localization [14], and arrest in quantum fluids [15]. Central questions in quantum many-body systems which display glassy behavior are understanding the interplay between static and dynamic properties [16], the relevance of quantum versus classical fluctuations [15,17], and the emergence of spatial correlations in the relaxation dynamics [18]. In this work, we take a first step toward addressing these issues from a dynamical facilitation perspective by introducing and studying a class of open quantum lattice systems that are the quantum analogs of classical facilitated spin models of glasses. These quantum spin systems, which are free of quenched disorder and have local interactions, display complex glassy dynamics despite the fact that their static properties are trivial. They also show a quantum version of dynamic heterogeneity, a feature we expect to be central to the dynamics of quantum glasses in general.

Quantum facilitated models.—Our aim is to construct a class of strongly interacting dissipative quantum many-body systems with the following two properties: firstly, interactions do not play an essential role in the statics and, as a consequence, the steady state of the system has the form of a direct product of single-site density matrices, like in a noninteracting problem; secondly, the interactions make the dynamics and, in particular, the relaxation to the steady state highly spatially correlated.

Consider the lattice system of Fig. 1. On each site $i = 1, \ldots, N$ there is a quantum two-level system, and we identify the two levels with basis states $|0\rangle_i$ and $|1\rangle_i$. These two levels are coupled coherently via an onsite Hamiltonian $h_i = \Omega\sigma_i^x$, where Ω is the coherent coupling strength and $\sigma_i^x \equiv |0\rangle_i\langle 1| + |1\rangle_i\langle 0|$. Each two-level system also interacts with a thermal bath that can cause incoherent excitation and deexcitation with rates γ and κ, respectively. In the absence of interaction between the sites,

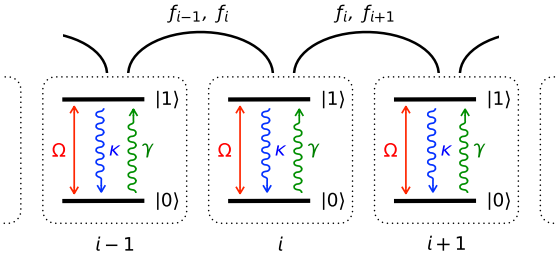

FIG. 1 (color online). Quantum facilitated models. A lattice of two-level systems with coherent and incoherent excitation or deexcitation. Interaction is via kinetic constraints f_i which make the rates on site i dependent on the state of its neighbors. The stationary state is trivial and non-interacting, while the dynamics is highly correlated and glassy when $\kappa \gg \Omega, \gamma$.

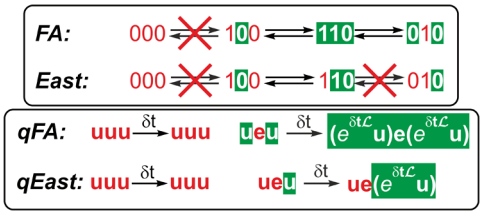

FIG. 2 (color online). Kinetic constraints. For the classical models, the upper panel shows three sites in a configuration, assuming all other sites are in the 0 state. For the quantum models, the bottom panel shows three sites of a product basis state for the density matrix, where we use the notation $\boldsymbol{u} \equiv |u\rangle\langle u|$ and $\boldsymbol{e} \equiv |e\rangle\langle e|$. Red (dark on white) symbols represent sites that cannot evolve. Green (white on dark) symbols represent sites where the state of neighboring sites allows for their evolution.

and under the standard Markovian approximation for the thermal bath [19], the open quantum dynamics of each site is described by the master equation

$$\dot{\rho}_i = \mathcal{L}_i(\rho_i) \equiv -i[h_i, \rho_i] + \kappa\sigma_i^- \rho_i \sigma_i^+ - \frac{\kappa}{2}\{\sigma_i^+\sigma_i^-, \rho_i\} + \gamma\sigma_i^+\rho_i\sigma_i^- - \frac{\gamma}{2}\{\sigma_i^-\sigma_i^+, \rho_i\}, \quad (1)$$

with $\sigma_i^\pm$ being the ladder operators defined in terms of the usual Pauli matrices as $\sigma_i^\pm = (\sigma_i^x \pm i\sigma_i^y)/\sqrt{2}$. This equation has as stationary solution $\rho_i^{(\mathrm{st})} \equiv \lambda_u |u\rangle_i\langle u| + \lambda_e |e\rangle_i\langle e|$, where the unexcited ($|u\rangle_i$) and excited ($|e\rangle_i$) states can be written as a superposition of $|0\rangle_i$ and $|1\rangle_i$, and $\lambda_{u,e}$ are their corresponding stationary occupation probabilities [20]. When the two-level systems are noninteracting, the stationary density matrix for the whole system is simply the direct product $\varrho_{\mathrm{ni}}^{(\mathrm{st})} = \bigotimes_{i=1}^N \rho_i^{(\mathrm{st})}$.

We now convert the system into an interacting problem with the the same trivial stationary state. We introduce interactions between nearest neighboring sites in the following manner: we condition the rates for both coherent and incoherent changes at the i-th site to the state of neighboring sites, i.e., $\Omega \to f_i\Omega$, $\kappa \to f_i\kappa$ and $\gamma \to f_i\gamma$, where f_i is a projection operator that acts only on the nearest neighbors of i, see Fig. 1. The many-body master equation now reads

$$\dot{\varrho} = \mathbb{W}(\varrho) \equiv -i[H, \varrho] + \sum_{i=1}^N \Big(L_i \varrho L_i^\dagger - \frac{1}{2}\{L_i^\dagger L_i, \varrho\} + J_i \varrho J_i^\dagger - \frac{1}{2}\{J_i^\dagger J_i, \varrho\} \Big) \quad (2)$$

with Hamiltonian and Lindblad [19] operators given by

$$H = \sum_{i=1}^N \Omega f_i \sigma_i^x, \quad L_i = \sqrt{\kappa} f_i \sigma_i^-, \quad J_i = \sqrt{\gamma} f_i \sigma_i^+. \quad (3)$$

The operators f_i represent kinetic constraints. Under certain general conditions for f_i [20], the stationary state of the interacting problem is the trivial one, i.e. $\varrho^{(\mathrm{st})} = \varrho_{\mathrm{ni}}^{(\mathrm{st})}$. We focus on two specific choices for the constraints that define the two models we study in detail (in dimension $d = 1$; $d > 1$ generalizations are immediate):

$$\mathrm{qFA}: f_i \equiv P_{i+1}^{(e)} + P_{i-1}^{(e)} - P_{i+1}^{(e)} P_{i-1}^{(e)} \quad (4)$$

$$\mathrm{qEast}: f_i \equiv P_{i+1}^{(e)}, \quad (5)$$

with $P_i^{(e)} \equiv |e\rangle_i\langle e|$ being projectors on the excited state on the i-th site.

The lattice models defined by Eqs. (2) and (3) are quantum versions of the facilitated spin models for classical glasses [10]. In particular, the choice of kinetic constraint (4) defines a quantum Fredrickson-Andersen (qFA) model [8,10], while that of (5) a quantum East (qEast) model [9,10]. The classical Fredrickson-Andersen (FA) and East models are recovered in the limit of vanishing coherent coupling, $\Omega = 0$. Figure 2 sketches the effect of the kinetic constraints. In analogy to the classical case, in both the qFA and qEast models, there can be no evolution in a site surrounded by unexcited neighbors [see Eqs. (4) and (5)]. In the qFA an excitation, like the central one in the rightmost sketch, facilitates both its neighbors which evolve with the single site master operator of Eq. (1). In contrast, in the qEast the central excitation can only facilitate dynamics to its right [21].

It is interesting to note that, in addition to the state $\varrho_{\mathrm{ni}}^{(\mathrm{st})}$, there is a second stationary state due to the kinetic constraints. This pure state, $\varrho^{(\mathrm{dark})} \equiv |u\cdots u\rangle\langle u\cdots u|$, is a "dark state" that is annihilated by the Hamiltonian and all the Lindblad operators independently, since $f_i \varrho^{(\mathrm{dark})} = \varrho^{(\mathrm{dark})} f_i = 0$ for all i. The dynamics defined by (2) and (3) is therefore reducible: It has one irreducible and "inactive" partition composed solely of $\varrho^{(\mathrm{dark})}$ and a second irreducible and "active" partition composed of everything else. In the thermodynamic limit, $N \to \infty$, the stationary state of the active partition becomes $\varrho^{(\mathrm{st})}$ up to corrections which vanish exponentially with N. In what follows we only consider dynamics in this partition.

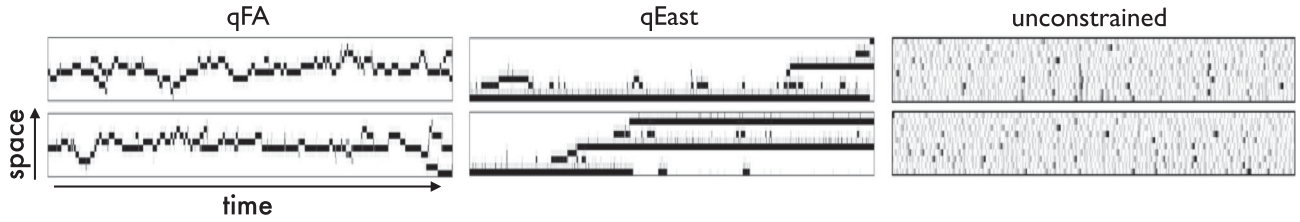

FIG. 3. Structure in trajectory space and dynamic heterogeneity. Quantum trajectories of the qFA, qEast, and unconstrained models, from QJMC simulations for $N = 10$ spins and periodic boundaries. We plot $\langle P_i^{(e)} \rangle(t) \in [0, 1] \equiv$ [white, black] for all sites $i = 1$ to N. The rates (κ, Ω, γ) for the trajectories shown are: (1, 0.25, 0) for the qFA and (1, 0.4, 0) for the qEast and the unconstrained ones. Space-time correlations are evident in the trajectories of the constrained models and absent in the unconstrained system.

Dynamical heterogeneity and slowdown of the relaxation.—We are interested in the dynamics of our quantum-facilitated spin models in the regime where the coherent coupling is weak and/or the temperature is low, i.e., $\kappa \gg \Omega, \gamma$. In this regime $\lambda_u \gg \lambda_e$ (see [20]), that is, the stationary state is such that very few sites are in the excited state $\boldsymbol{e}$. This, however, leads to a conflict with the dynamics, as the kinetic constraint on a site vanishes unless some of its neighbors are in the excited state, and in this regime most sites will be surrounded by unexcited sites. The consequence is a pronounced slowdown and the emergence of collective dynamics.

Let us consider how excitations propagate in the quantum models we propose. Typically, at low Ω/κ, γ/κ, excitations will be isolated. We denote a state with such an excitation by $\cdots \boldsymbol{ueu} \cdots$ (see Fig. 2). As we have explained, the isolated excited site cannot evolve, but it can facilitate evolution of its neighbors. Let us first consider the case of the qFA model: here, the initial excitation can facilitate the excitation of either of the neighboring sites. This new excitation subsequently facilitates the original site, which can now deexcite. The first process could be either virtual or real, and it is limited by the rates Ω or γ. The second process will be dominated by incoherent deexcitation with rate κ. In the classical limit, the outcome of such sequence is that an isolated excitation hops one site. In the qFA model, excitations also propagate diffusively, with an effective diffusion constant that vanishes in the limit Ω/κ, $\gamma/\kappa \to 0$, in analogy to the classical FA model at low temperatures [10]. Dynamics of the qEast model is even more complex. Because of the directionality of the kinetic constraint, Eq. (5), the last step in the hopping sequence sketched above is not allowed and the relaxation is therefore hierarchical [2,10].

Figure 3 shows examples of quantum trajectories from quantum jump Monte Carlo (QJMC) simulations [22]. The trajectories for the qFA clearly show the diffusive nature of the dynamics: when initialized from a single site in the $|e\rangle$ state and the rest in the $|u\rangle$, this initial excitation propagates in a diffusive manner. Occasionally, excitations branch out or coalesce. Because of the kinetic constraints, excitations have to form connected chains in space and time [2], as illustrated in the figure. The hierarchical relaxation dynamics of the qEast model is also observed in the trajectories of Fig. 3. For comparison, we also show trajectories under similar conditions for the unconstrained problem [see Eq. (1)]. These trajectories are featureless, as there is no interaction between the sites, which then evolve independently. Note that all three systems shown in Fig. 3 possess the same stationary properties, despite the fact that their dynamics (and the approach to such stationary states) is obviously different. The quantum trajectories of Fig. 3 are qualitatively similar to those of the corresponding classical models, see, e.g., Fig. 2 of Ref. [23]. This is despite the fact that the trajectories shown are fully quantum (i.e., this is not semiclassics). A remarkable aspect is that while one would expect the quantum dynamics to lead to excitations that are smeared out, an initial localized excitation remains localized at each time. Furthermore, one of our central messages is that quantum glassy relaxation should lead to dynamical heterogeneity. The quantum trajectories of Fig. 3 directly illustrate this feature.

The effective diffusion constant for propagation of excitations in the qFA model can be estimated analytically when $\Omega, \gamma \ll \kappa$ by carrying out an adiabatic elimination of fast degrees of freedom, or by numerical simulation of the evolution operator (2) in small lattices (see Supplemental Material [20]). These results suggest that the diffusion constant reads

$$D = \left(\frac{\gamma}{2} - \frac{\gamma^2}{6\kappa}\right) - \frac{4\Omega^2}{\kappa^2}\left(\gamma - \frac{2\gamma^2}{\kappa}\right) + \frac{8\Omega^4}{\kappa^3} + \cdots \qquad (6)$$

In the limit of zero temperature, $\gamma = 0$, the diffusion constant is $D = 8\Omega^4/\kappa^3$ to leading order in Ω. Relaxation of a site initially in an unexcited state will depend on how long it takes for the nearest excitation to diffuse to it. If the distance is l, then the time to relax will be $\tau(l) \approx l^2/D$. Figure 4(a) shows that this diffusive argument accounts very well for the relaxation time τ_{relax} obtained from QJMC simulations in the qFA model. As expected, the relaxation slows down very markedly with the decrease of quantum fluctuations. The inset to Fig. 4(a) shows that the relaxation time in the qEast model grows with decreasing Ω even faster than in the qFA as a consequence of the more restrictive kinetic constraints.

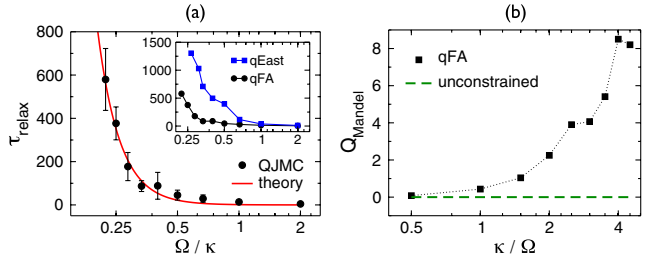

FIG. 4 (color online). Glassy slowing down and dynamical correlations. (a) Average relaxation time τ_{relax} as a function of Ω/κ (at $\gamma = 0$) in the qFA model. The dots are results from QJMC simulations. The line is the theoretical expectation for relaxation via activated diffusion of excitations: since the initial state has a single excitation, in a lattice of size N with periodic boundary conditions we expect $\tau_{\text{relax}} \approx (2/N)\sum_{l=1}^{N/2} \tau(l)$. Inset: τ_{relax} for the qEast model. (b) Fluctuations in waiting times between quantum jump events for the same qFA system, quantified via Q_{Mandel}.

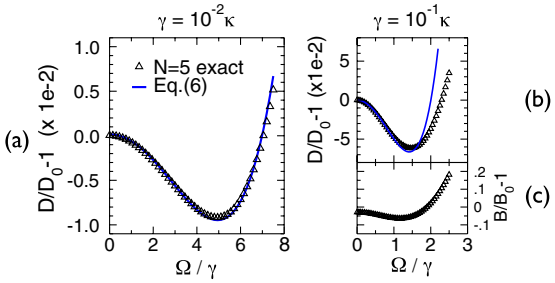

FIG. 5 (color online). Enhanced glassiness due to weak quantum fluctuations. Effective diffusion constant D in the qFA model at $\gamma \neq 0$. Panels (a) and (b) show D for the cases of $\gamma = 10^{-2}\kappa$ and $10^{-1}\kappa$. As γ and Ω become larger compared to κ, the analytic approximation (6) becomes less quantitatively accurate, as expected, but reentrance is still evident from the exact result. Panel (c) shows similar reentrance behavior of the branching rate B. D_0 and B_0 are the classical values of the diffusion constant and the branching rate, respectively.

From the trajectories of the qFA and qEast shown in Fig. 3, we see that, in the constrained cases considered, when the dynamics is slow it is also heterogeneous. Regions of space empty of excitations are slow to relax, as they need excitations external to the region to propagate into it for the dynamics to take place. The larger these empty regions, the longer they take to evolve. These slow "space-time bubbles" [23] make the dynamics fluctuation dominated. Just like the existence of a dark state $\varrho^{(\text{dark})}$, space-time bubbles are a consequence of the kinetic constraints: mesoscopic regions devoid of excitations look locally like the dark state and can only become dynamical from their outside. At low Ω/κ, γ/κ, these spatial rare regions give rise to dynamic heterogeneity.

A manifestation of dynamic heterogeneity is in the fluctuations of the waiting times t_w between quantum jump events in each site. When the dynamics is spatially correlated, quantum jumps are non-Poissonian and the corresponding distribution of waiting times is nonexponential. This can be quantified by the Mandel-Q parameter for the waiting times, $Q_{\text{Mandel}} \equiv \langle t_w^2\rangle/\langle t_w\rangle^2 - 2$ [24]. For correlated (bunched) quantum jumps, we have that $Q_{\text{Mandel}} > 0$, indicating that the fluctuations in the waiting times can be much larger than what is expected from a Poisson process. Figure 4(b) shows that this is the case for the qFA model. In the glass literature, this is often referred to as "decoupling" [2,5].

Interplay of quantum and classical fluctuations.—For the system to relax, it is necessary to excite sites, which can be done incoherently with rate γ or coherently with rate Ω. It would, then, seem that adding quantum fluctuations to a classical facilitated system should always aid relaxation, but this is not the case. From Eq. (6), we see that in the qFA model, for γ, $\Omega \ll \kappa$, the first correction to the classical diffusion constant is negative, and only for larger Ω do quantum contributions become positive; see Fig. 5. This means that weak quantum fluctuations enhance dynamical arrest by decreasing the propagation rate of excitations. Figure 5(c) shows that this also holds for the rate B for branching of excitations. Similar reentrance is present in other quantum facilitated models, such as the qEast. This is because the first effect of quantum fluctuations is to make the classical basis 0,1 different from the quantum basis $\boldsymbol{u}$, $\boldsymbol{e}$; one can think of this as a rotation by an angle proportional to Ω [20]. A classical excitation collapses the wave function on a site to the 1 state, but in the $\boldsymbol{u}$, $\boldsymbol{e}$ basis this is not just an excitation, $\boldsymbol{e}$, but also a projection onto $\boldsymbol{u}$. Thus, to order Ω^2, the uncertainty due to quantum fluctuations has the effect of making a classical excitation not as efficient as it would be in the absence of quantum effects; only at order Ω^4 do quantum fluctuations give an effective speed-up in relaxation. This phenomenon of enhanced glassiness due to weak quantum fluctuations near the classical limit appears to be similar to that reported recently for glass-forming quantum liquids in Ref. [15].

Outlook.—We expect the dynamics of glassy quantum many-body systems with local interactions to display the essential feature of the idealized models we introduced in this Letter, namely a spatially fluctuating and heterogeneous dynamics that cannot be simply inferred from static behavior. To understand this correlated dynamics, one would need to uncover the effective kinetic constraints. In this sense, we envisage quantum facilitated models as an effective description of the more complex glassy many-body quantum dynamics. Given the recent progress in quantum many-body physics with cold atoms, it may be possible to directly implement and study constrained models in experiments. For example, Rydberg atoms [25] exhibit strong interactions that have been shown to lead to constraints in the coherent dynamics [26–28] that, in conjunction with atomic decay, can give rise to pattern formation in quantum jump trajectories [29]. Furthermore, recent work focusing on the engineering of system-bath coupling [30,31] outlines a path for

devising the constrained many-body jump operators required by the models presented here.

This work was funded in part by EPSRC Grant No. EP/I017828/1 and Leverhulme Trust Grant No. F/00114/BG. B. O. also acknowledges funding by Fundación Ramón Areces.

[1] A. Cavagna, Phys. Rep. **476**, 51 (2009).
[2] D. Chandler and J. P. Garrahan, Annu. Rev. Phys. Chem. **61**, 191 (2010).
[3] L. Berthier and G. Biroli, Rev. Mod. Phys. **83**, 587 (2011).
[4] K. Binder and W. Kob, *Glassy Materials and Disordered Solids* (World Scientific, Singapore, 2011).
[5] For reviews on dynamical heterogeneity, see M. D. Ediger, Annu. Rev. Phys. Chem. **51**, 99 (2000); H. C. Andersen, Proc. Natl. Acad. Sci. U.S.A. **102**, 6686 (2005).
[6] For thermodynamic perspectives on glasses see, for example D. Kivelson *et al.*, Physica (Amsterdam) **219A**, 27 (1995); P. Debenedetti and F. Stillinger, Nature (London) **410**, 259 (2001); V. Lubchenko and P. G. Wolynes, Annu. Rev. Phys. Chem. **58**, 235 (2007).
[7] R. G. Palmer, D. L. Stein, E. Abrahams, and P. W. Anderson, Phys. Rev. Lett. **53**, 958 (1984).
[8] G. H. Fredrickson and H. C. Andersen, Phys. Rev. Lett. **53**, 1244 (1984).
[9] J. Jäckle and S. Eisinger, Z. Phys. B **84**, 115 (1991).
[10] F. Ritort and P. Sollich, Adv. Phys. **52**, 219 (2003).
[11] G. Biroli, C. Chamon, and F. Zamponi, Phys. Rev. B **78**, 224306 (2008).
[12] A. Das and B. K. Chakrabarti, Rev. Mod. Phys. **80**, 1061 (2008).
[13] A. Amir, Y. Oreg, and Y. Imry, Phys. Rev. Lett. **103**, 126403 (2009).
[14] A. Pal and D. A. Huse, Phys. Rev. B **82**, 174411 (2010).
[15] T. E. Markland, J. A. Morrone, B. J. Berne, K. Miyazaki, E. Rabani, and D. R. Reichman, Nature Phys. **7**, 134 (2011).
[16] C. Chamon, Phys. Rev. Lett. **94**, 040402 (2005).
[17] L. Foini, G. Semerjian, and F. Zamponi, Phys. Rev. B **83**, 094513 (2011).
[18] Z. Nussinov, Physics **1**, 40 (2008).
[19] C. W. Gardiner and P. Zoller, *Quantum Noise* (Springer-Verlag, Berlin, 2004).
[20] See Supplemental Material at http://link.aps.org/supplemental/10.1103/PhysRevLett.109.020403 for technical details.
[21] For an earlier attempt at defining a semiclassical quantum East model, see A. Das, B. K. Chakrabarti, and R. B. Stinchcombe, Phys. Rev. E **72**, 026701 (2005).
[22] M. B. Plenio and P. L. Knight, Rev. Mod. Phys. **70**, 101 (1998).
[23] J. P. Garrahan and D. Chandler, Phys. Rev. Lett. **89**, 035704 (2002).
[24] E. Barkai, Y. J. Jung, and R. Silbey, Annu. Rev. Phys. Chem. **55**, 457 (2004).
[25] T. Gallagher, *Rydberg Atoms* (Cambridge University Press, Cambridge, 1984).
[26] I. Lesanovsky, Phys. Rev. Lett. **106**, 025301 (2011).
[27] S. Ji, C. Ates, and I. Lesanovsky, Phys. Rev. Lett. **107**, 060406 (2011).
[28] C. Ates and I. Lesanovsky, arXiv:1202.2012 [Phys. Rev. A (to be published)].
[29] T. E. Lee and M. Cross, Phys. Rev. A **85**, 063822 (2012).
[30] S. Diehl, A. Micheli, A. Kantian, B. Kraus, H. P. Büchler, and P. Zoller, Nature Phys. **4**, 878 (2008).
[31] S. Diehl, W. Yi, A. J. Daley, and P. Zoller, Phys. Rev. Lett. **105**, 227001 (2010).